Neurobiology of Disease

Fukutin-Related Protein Alters the Deposition of Laminin in the Eye and Brain

Mark R. Ackroyd,[1] Charlotte Whitmore,[1,2] Sarah Prior,[1] Manuja Kaluarachchi,[1] Margareta Nikolic,[2] Ulrike Mayer,[3] Francesco Muntoni,[4] and Susan C. Brown[1]

[1]Department of Veterinary Basic Sciences, Royal Veterinary College, University of London, London NW1 0TU, United Kingdom, [2]Wolfson Neuroscience Laboratories, Department of Medicine, Imperial College, London, London W12 0NN, United Kingdom, [3]Biomedical Research Centre, School of Biological Sciences, University of East Anglia, Norwich NR4 7TJ, United Kingdom, and [4]Institute of Child Health, University College London, London WC1N 1EH, United Kingdom

Mutations in fukutin-related protein (FKRP) are responsible for a common group of muscular dystrophies ranging from adult onset limb girdle muscular dystrophies to severe congenital forms with associated structural brain involvement. The defining feature of this group of disorders is the hypoglycosylation of α-dystroglycan and its inability to effectively bind extracellular matrix ligands such as laminin α2. However, α-dystroglycan has the potential to interact with a number of laminin isoforms many of which are basement membrane/tissue specific and developmentally regulated. To further investigate this we evaluated laminin α-chain expression in the cerebral cortex and eye of our FKRP knock-down mouse (FKRP^{KD}). These mice showed a marked disturbance in the deposition of laminin α-chains including α1, α2, α4, and α5, although only laminin α1- and γ1-chain mRNA expression was significantly upregulated relative to controls. Moreover, there was a diffuse pattern of laminin deposition below the pial surface which correlated with an abrupt termination of many of the radial glial cells. This along with the pial basement membrane defects, contributed to the abnormal positioning of both early- and late-born neurons. Defects in the inner limiting membrane of the eye were associated with a reduction of laminin α1 demonstrating the involvement of the α-dystroglycan:laminin α1 axis in the disease process. These observations demonstrate for the first time that a reduction in *Fkrp* influences the ability of tissue-specific forms of α-dystroglycan to direct the deposition of several laminin isoforms in the formation of different basement membranes.

Introduction

A number of forms of congenital muscular dystrophy are now known to be associated with mutations in genes that encode for proteins implicated in the glycosylation and/or processing of α-dystroglycan (Michele and Campbell, 2003; Muntoni et al., 2004; Barresi and Campbell, 2006). Mutations in *POMT1* (Beltrán-Valero de Bernabé et al., 2002), *POMT2* (van Reeuwijk et al., 2005), *POMGnT1* (Yoshida et al., 2001), *LARGE* (Grewal and Hewitt, 2002; Longman et al., 2003; van Reeuwijk et al., 2007), *FKRP* (fukutin-related protein) (Brockington et al., 2001a,b; Beltran-Valero de Bernabé et al., 2004), and *Fukutin* (Toda, 1999) are all typically associated with a wide clinical spectrum. In Caucasian populations mutations are most frequently seen in the *FKRP* gene (Muntoni et al., 2008). The characteristic and diagnostic feature of all of these variants is the hypoglycosylation of α-dystroglycan, hence the term "dystroglycanopathies" for this group of disorders (Toda et al., 2003; Godfrey et al., 2007; Muntoni et al., 2007; Clement et al., 2008a). The severe end of the clinical spectrum is likely to be associated with very low or undetectable levels of functional FKRP, as suggested by a recent report of a homozygous *FKRP* initiation codon mutation with Walker-Warburg syndrome (van Reeuwijk et al., 2010).

Dystroglycan has been attributed with a primary role in the deposition, organization and turnover of basement membranes (Durbeej et al., 1995; Henry and Campbell, 1998; Henry et al., 1998; Michele et al., 2002; Yurchenco et al., 2004a,b). The glycan chains of the central mucin domain of α-dystroglycan are known to mediate binding to components such as laminin (Ervasti and Campbell, 1993), perlecan (Peng et al., 1998) agrin (Bowe et al., 1994; Campanelli et al., 1994; Gee et al., 1994), neurexin in the brain (Sugita et al., 2001) and pikachurin in the eye (Sato et al., 2008). Aberrant glycosylation of α-dystroglycan is thought to be central to the pathogenesis of the muscular dystrophy and the brain abnormalities manifested by patients (cobblestone lissencephaly) and animal models with severe forms of dystroglycanopathy (Michele et al., 2002; Michele and Campbell, 2003; Hewitt, 2009; Yoshida-Moriguchi et al., 2010).

We have previously generated mice with an 80% reduction in *Fkrp* transcript levels (FKRP knock-down or FKRP^{KD}) (Ackroyd et al., 2009) and now use these mice to show that a reduction in

Received May 9, 2011; revised June 30, 2011; accepted July 14, 2011.

Author contributions: M.R.A., C.W., and S.C.B. designed research; M.R.A., C.W., S.P., and M.K. performed research; M.N. and U.M. contributed unpublished reagents/analytic tools; M.R.A., C.W., M.N., F.M., and S.C.B. analyzed data; M.R.A. and S.C.B. wrote the paper.

We gratefully acknowledge the support of the Association Francaise contres les Myopathies (AFM) and the Muscular Dystrophy Association of America (MDA). F.M. is supported by Great Ormond Street Hospital Children's Charity. We also thank Drs. Anita Hall and Jane Saffell for their helpful discussions during the course of this work.

The authors declare no competing financial interests.

Correspondence should be addressed to Susan C. Brown, Department of Veterinary Basic Science, Royal Veterinary College, University of London, London NW1 0TU, UK. E-mail: scbrown@rvc.ac.uk.

DOI:10.1523/JNEUROSCI.2301-11.2011

 0270-6474/11/3112927-09$15.00/0

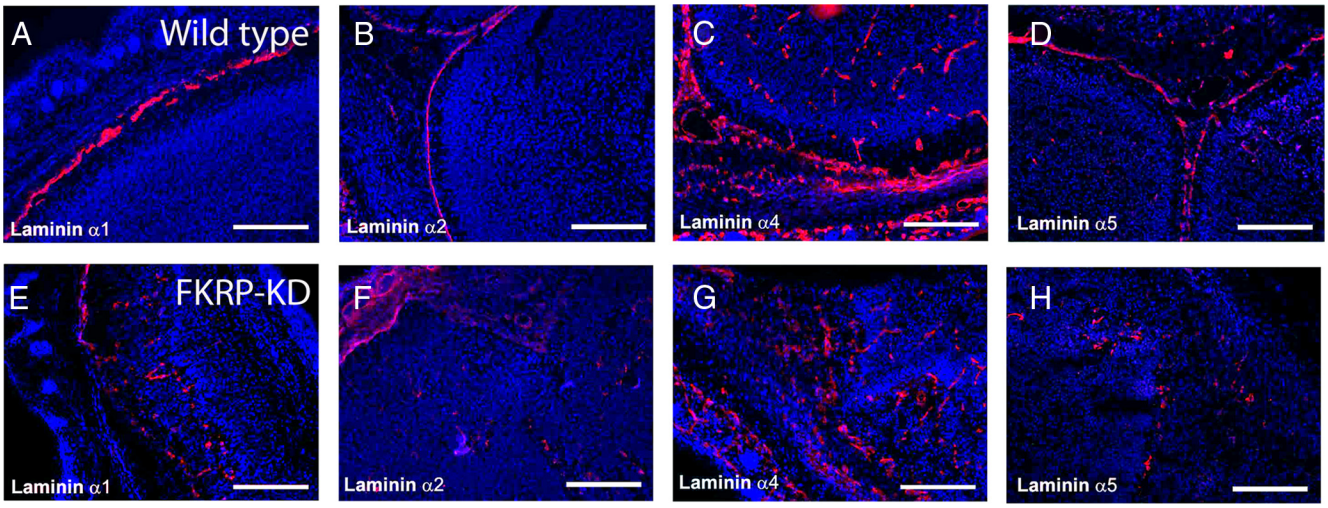

Figure 1. Irregular laminin α-chain deposition in the cerebral cortex of FKRP^{KD} mice. ***A–H***, Coronal sections (20 μm) of the cerebral cortex of newborn wild-type (***A–D***) and FKRP^{KD} (***E–H***) mice were stained with a panel of laminin α-chain antibodies. Comparable sections were selected for both the mutants and controls at levels where the left and right hemispheres are juxtaposed and the central hemispheric fissure was clearly present. Laminin α1 immunostaining is mislocalized across the cerebral cortex in the FKRP^{KD} brain (***E***) compared with wild-type (***A***) where laminin α1 staining is strictly localized to the pial surface. Laminin α2 and α5 immunostaining is significantly reduced at the pial surface in the FKRP^{KD} brain (***F***, ***H***) compared with wild-type controls (***B***, ***D***). Laminin α4 staining is present in the vasculature in both the mutants and controls (***C***, ***G***) but the staining pattern at the pial surface is highly disorganized in the FKRP^{KD} brain. Scale bars, 50 μm.

Fkrp leads to a marked disturbance in the deposition of several laminin α-chains in the brain which subsequently contributes to a disruption of the radial glial scaffold and neuronal positioning. Laminin chain expression showed a significant increase in laminin α1 and γ1 transcripts in the newborn brain of the FKRP^{KD} compared with controls. Breaches of the inner limiting membrane (ILM) of the eye were associated with a reduction in laminin α1, thus demonstrating for the first time the role of laminin α1 in the pathogenesis of this group of disorders. These observations are consistent with the glycosylation of α-dystroglycan playing a central role in the incorporation of laminin into basement membranes but highlight tissue-specific differences in basement membrane formation which have a clear impact on the tissue-specific phenotypes observed.

Materials and Methods

Generation and breeding of FKRP-Neo^{Tyr307Asn} *mice.* We generated *FKRP-Neo*^{Tyr307Asn} lines of mice (henceforth referred to as FKRP^{KD}), which contained in addition to the knock-in mutation, a Neo^{R} cassette in intron 2. In both lines the number of homozygote mice born was ~25%, consistent with there being no embryonic lethality.

Immunohistochemistry. Muscle and brain samples were frozen in isopentane cooled in liquid nitrogen. Cryostat sections were labeled with rat anti-laminin α1 (Sorokin et al., 1992), rat anti-laminin α2 (4H8, Abcam), rabbit anti-laminin α4 (R&D Systems), anti-laminin α5 (kind gift from Jeffrey Miner, Washington University School of Medicine, St. Louis, MO), rat anti-laminin γ1 (clone A5; Millipore), and laminin (Sigma) followed by anti-rat/rabbit/mouse tagged with Alexa Fluor 488 or 594 (Invitrogen) for 30 min. IIH6 and RC2 (Developmental Studies Hybridoma Bank, Iowa) were labeled with anti-IgM biotinylated antibody (1 h) followed by streptavidin conjugated with Alexa Fluor 594. Nuclei were stained with Hoechst 33342 (Sigma). All dilutions and washings were made in PBS. Sections were mounted in aqueous mountant and viewed with epifluorescence using a Nikon E1000M microscope. Images were digitally captured with CoolSnap HQ (Photometrics) CCD monochrome camera using a Image Pro Plus Imaging system. All images were compiled using Photoshop CS (Adobe). Where direct comparisons have been made fluorescent images were captured with equal exposure and have had equal scaling applied. All observations are based on a minimum of $n = 3$ (of either sex), representative images are shown.

RT-PCR analysis. Brain and muscle were dissected out and homogenized with liquid nitrogen using a mortar and pestle and the lysate passed through a QiaShredder (Qiagen). The RNA was isolated from the homogenized tissue using an RNeasy kit (Qiagen) and for muscle RNeasy Fibrous Tissue Kit (Qiagen) eluted with 30 μl RNase free H_2O. RNA (1 μg) was reverse transcribed with SuperscriptIII Platinum for qRT-PCR kit (Invitrogen). qRT-PCR was performed on a 7500 FAST Real-Time PCR system (Applied Biosystems) using a FAM reporter dye system for each reaction 0.8 μl of cDNA was used as template in a PCR mix consisting of 1 μl of primer mix, 10 μl of TaqMan Universal PCR Mastermix (Applied Biosystems), and 8.2 μl of H_2O. The primers for the gene expression assays were sourced commercially from Applied Biosystems (*FKRP* Mm00557870_mL, *Lama1* Mm00439481_m1, *Lama2* Mm01193193_m1, *Lama3* Mm01254761_m1, *Lama4* Mm01193657_m1, *Lama5* Mm01222051_g1, *Lamc1* Mm00711817_g1, *GAPDH* Mm99999915_gL). Each experiment represents a minimum of $n = 3$ (of either sex) and all reactions were performed in triplicate.

Distribution of transcription factor and Ki67-labeled nuclei in the neocortex. Cryosections (12 μm) of newborn brains were stained for a variety of molecular markers and counterstained for DAPI. For each molecular marker (and DAPI-stained nuclei to calculate total nuclei across the cortex) three transverse sections selected from either the *FKFP*^{KD} mice and or control littermates were examined. The distance from the ventricular zone to the pial basement membrane was divided into 6 equal regions. The number of positively stained nuclei were then counted within each layer and expressed as a percentage of the total number of nuclei to illustrate the distribution of nuclei across the cortex. Three similar regions from serial sections of the neocortex were counted for each littermate and each experiment represents a minimum of $n = 3$ (of either sex). Statistical analysis was performed using a two-tailed t test in GraphPad (Prism).

Detection of apoptosis in the cortex. Cryosections (12 μm) of newborn brains were labeled with ApopTagFluorescein Direct In Situ Apoptosis Detection Kit (Millipore) and the percentage of positively stained nuclei within a slice extending from the ventricular zone to the pial basement membrane was calculated relative to the total number of Hoechst-stained nuclei. Counts were based on $n = 3$ for both FKRP^{KD} and wild-type

controls (of either sex). Statistical analysis was performed using a two-tailed *t* test in GraphPad (Prism).

Results

Laminin deposition is disturbed during cortical development in FKRP^{KD} mice

We previously noted a reduction in laminin α2 at the pial basement membrane of newborn FKRP^{KD} mice. To determine whether the expression of other laminin α-chains was similarly affected and contributed to the phenotype we used antibodies specific to laminin α1, α4, and α5. Labeling for laminin α1 and α5 but not α4 was found to be reduced at the pial basement membrane and all three α-chains highlighted a discontinuous basement membrane. However, there was an irregular pattern of deposition of laminin α1 below the pial surface in the superficial areas of the cerebral cortex which suggested an overall increase in laminin αl. This irregular pattern of staining was never observed in any of the wild-type controls examined (Fig. 1).

It has previously been suggested that cerebellar granule cell migration may be influenced by punctate deposits of laminin generated by radial glial cells (Liesi, 1990). Consequently we sought to determine the relationship between this disturbed distribution of laminin α1 deposition and the altered radial glial cell scaffold. Double labeling of the FKRP^{KD} neocortex with RC2, an intermediate filament protein expressed in radial glial cells, and laminin α1 showed that while occasional radial glial cells made direct contact with the pial basement membrane as in wild-type mice, the majority did not extend this far with a proportion of these terminating at sites of irregular laminin α1 deposition (Fig. 2). Interestingly, α-dystroglycan was undetectable at these sites of interaction at this time point suggesting that the endfeet may be interacting with laminin via another receptor.

Cells commonly undergo apoptosis if unable to make attachments to the basement membrane, however, comparisons of the incidence of apoptotic nuclei in the cortical plate of newborn FKRP^{KD} and wild-type mice showed no significant differences (1.38 $\pm$ 1.1% SEM) and 0.85 $\pm$ 0.4% (SEM), respectively. This suggests that an alteration in the rate of apoptosis in the newborn brain does not contribute to the brain phenotype observed in this model.

The migration of early- and late-born neurons is disturbed in FKRP^{KD} mice

To determine whether the position of early-born neurons is altered in the FKRP^{KD} mouse, we immunolabeled for transcription factors that identify neurons in the ventricular and subventricular zone (Tbr-2) (Englund et al., 2005), layer VI (Tbr-1) (Hevner et al., 2001) and layer V (Ctip2) (Leid et al., 2004) (Fig. 3*A*,*B*). Ctip2-labeled neurons localized to a distinct region (zone 5) in the wild-type cortices. However, in the FKRP^{KD} cortex there was no clear lamination of the Ctip2-labeled cells which were instead found to be distributed across the cortical plate (Fig. 3*A*). Neurons destined to form Layer VI as identified by the transcription factor Tbr-1, were more widely distributed across the cortex with no distinct lamination in contrast to wild-type controls (Fig. 3*B*). There was no significant difference between wild-type controls and FKRP^{KD} mice with respect to the number or distribution of Tbr-2-positive neurons (Fig. 3*A*). Ki67 is a marker of proliferating cells. No statistically significant difference in the total number of Ki67-positive cells was noted between wild-type and FKRP^{KD} mice ($p = 0.6$) although there appeared to be more Ki67-positive cells located close to the marginal zone in the FKRP^{KD} compared with wild-type controls (Fig. 3*A*).

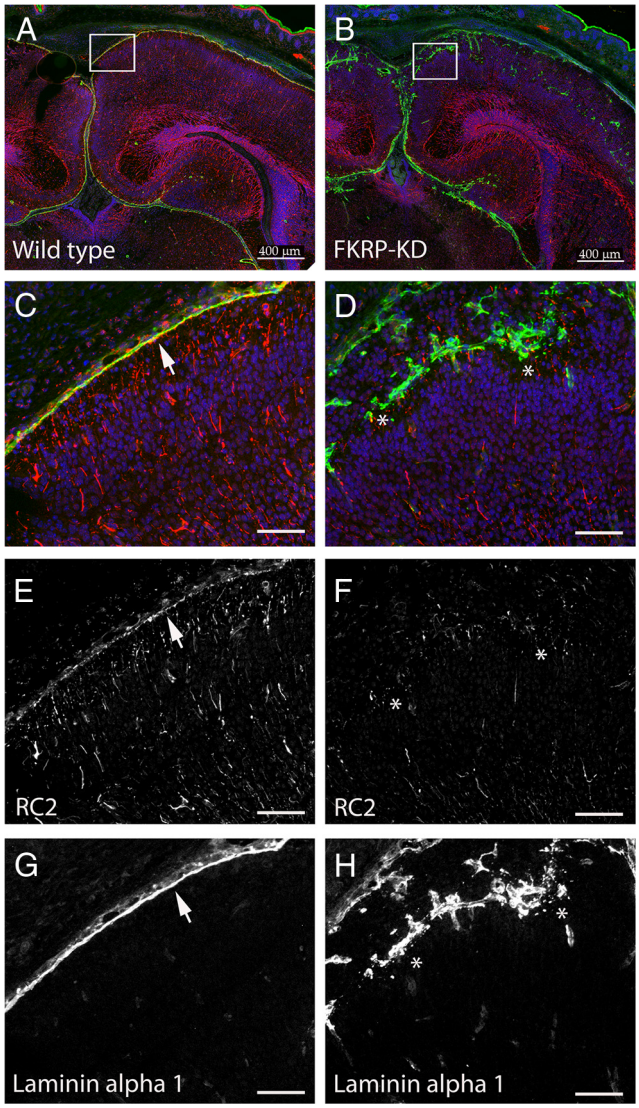

Figure 2. Radial glial endfeet associate with aberrantly localized laminin α1 in the FKRP^{KD} mice. ***A–H***, Coronal sections (20 μm) of the cerebral cortex of newborn wild-type (***A***, ***C***, ***E***, ***G***) and FKRP^{KD} mice (***B***, ***D***, ***F***, ***H***) were immunolabeled with laminin α1 (green) and RC2, a marker for radial glia (red). Nuclei are counterstained with Hoechst 33342 (blue). Laminin α1 immunostaining can be observed throughout the cortex in the FKRP^{KD} cortex (***B***) compared with wild-type (***A***) where laminin α1 is restricted to the pial basement membrane. In the wild-type mice the radial glia endfeet form the glial limitans (arrows) and colocalize with laminin α1 at the pial surface. In the FKRP^{KD} the radial glial endfeet do not form a continuous glial limitans at the pial surface and their endfeet can often be observed juxtaposed with the mislocalized laminin α1 (*). ***C–H*** represent enhanced regions of ***A*** and ***B***, indicated by white boxes. Individual channels for RC2 (***E***, ***F***) and laminin α1 (***G***, ***H***) are shown. Scale bars: ***A***, ***B***, 400 μm; ***C–H***, 50 μm.

To investigate the migration pattern of late-born neurons we injected pregnant females with BrdU at 15.5 d gestation [embryonic day 15.5 (E15.5)] and the brains of newborn mice were examined at postnatal day 0 (P0). This protocol identified neurons that were in S phase at E15.5 which in the wild-type controls showed migration across the cortical plate toward the marginal zone while the same population of cells in FKRP^{KD} mice accumulated midway across the cortical plate (Fig. 3*B*). These observations clearly indicate that the radial glial scaffold was defective at or by the time that these neurons were required to migrate across the cortex.

Since the cortical plate has not fully developed at P0 we arbitrarily divided the cortex into 6 equal regions with zone 1 being closest to

the ventricular zone and zone 6 adjacent to the pial basement membrane (as illustrated in Fig. 4*A*). There was no significant alteration in the total number of cortical nuclei between FKRP^{KD} mice and wild-type controls or in the populations of Tbr2- or Ctip2-labeled neurons, although the distribution of Ctip2-labeled neurons was disrupted (Fig. 4). In contrast however, the population of Tbr1-labeled neurons (Fig. 4*C*) was significantly decreased in the cortex of the FKRP^{KD} mice ($p = 0.0274$, two-tailed *t* test).

Basement membranes of the eye are altered by reduced Fkrp expression

We have previously noted a disturbance in the ILM of the FKRP^{KD} mouse despite our observations that neither laminin α2 nor glycosylated α-dystroglycan are present at this basement membrane in the wild-type newborn retina. Laminin α1 was the only laminin α-chain that was detected at the ILM (Fig. 5). It is noteworthy that we were unable to detect either laminin α4 or α5 at the ILM. Laminin α1 was observed in both the wild-type controls and FKRP^{KD} retinas; however, the integrity of the ILM was found to be markedly disturbed in the FKRP^{KD} relative to that of wild-type, as indicated by the discontinuous staining pattern of the laminin α1 antibody (Fig. 5). Antibodies specific for laminin α1 and laminin-111/211 revealed that the ILM is disturbed in the FKRP^{KD} retina compared with wild-type. Ectopic cells of the retinal ganglion cell layer were observed in the vitreous of the mutant eye (Fig. 5). Furthermore, costaining with laminin α1 and RC2 (which is expressed in the Müller glia) clearly illustrated that the Müller glia endfeet penetrated through the ILM into the vitreous body in the FKRP^{KD} mice (Fig. 5).

The glycosylation of α-dystroglycan at the ILM is developmentally regulated

We have previously published that the glycosylated epitope of α-dystroglycan, as indicated by IIH6 staining, was undetectable at the ILM of wild-type newborn mouse eyes (Ackroyd et al., 2009). We therefore investigated whether the IIH6 epitope was present at the ILM during the development of the eye. Immunostaining with IIH6 and laminin antibodies clearly demonstrated that the IIH6 epitope is present at both the ILM and Bruch's membrane of E12.5 wild-type retinas (Fig. 6). As previously reported no IIH6 immunoreactivity was detectable in the wild-type newborn eye despite it being present at the sarcolemma of the extraocular muscle (Fig. 6). IIH6 immunoreactivity was also undetected at the ILM of E15.5 wild-type eyes (Whitmore et al., 2011). These results clearly demonstrate that the glycosylation of α-dystroglycan is developmental regulated in the eye and suggests that this glycosylation is necessary in the formation, if not the maintenance of the basement membranes of the mouse retina.

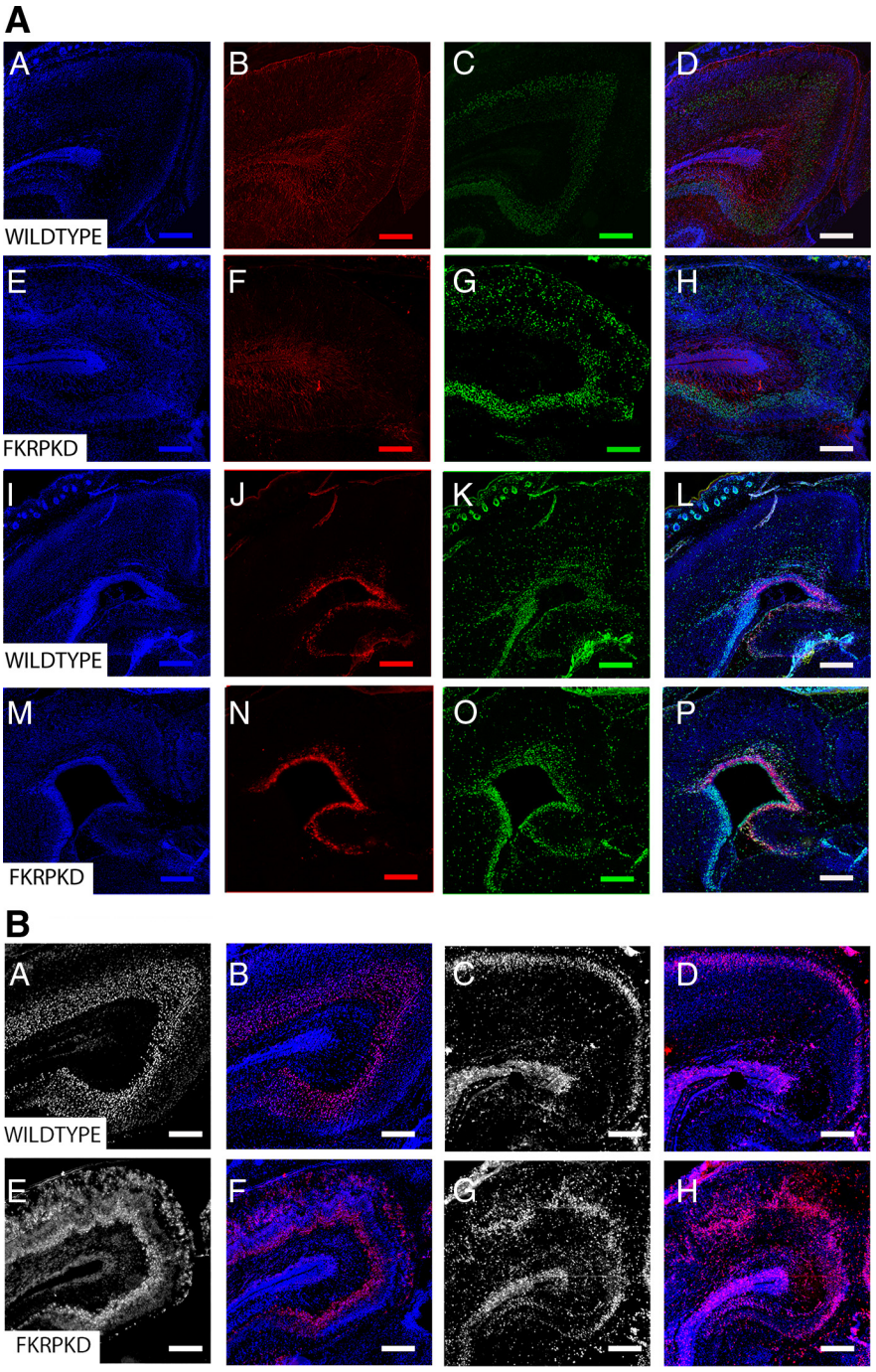

Figure 3. ***A***, Neuronal migration in the cerebral cortex of the FKRP^{KD} mice. ***A–P***, Coronal sections (20 μm) of the cerebral cortex from wild-type (***A***, ***D***, ***I–L***) and FKRP^{KD} mice (***E–H***, ***M–P***). Comparable sections were selected in both the mutants and controls at the midline of the cerebral cortex where the left and right hemispheres are juxtaposed. ***A–H*** illustrate representative images of cortices costained with Hoechst 33342 (blue), to label the nuclei (***A***, ***E***); RC2 (red), a marker for radial glia (***B***, ***F***); and Ctip2 (green), a transcription factor expressed in layer V neurons (***C***, ***G***). ***D*** and ***H*** illustrate a merged image of tiles ***A–C*** and ***E–G***, respectively. ***I–L*** and ***M–P*** represent cortices immunolabeled for Tbr-2 (red), a transcription factor expressed in cells of the subventricular zone (***J***, ***N***) and Ki67 (green), to label proliferating cells. Hoechst 33342 was used to counterstain the nuclei (blue; ***I***, ***M***) and the merged image is shown (***L***, ***P***). Scale bars, 200 μm. ***B***, Coronal sections (20 μm) of the cerebral cortex from wild-type (***A–D***) and FKRP^{KD} mice (***E–H***). Layer VI neurons were labeled with antibodies against Tbr-1 (***A***, ***E***). Images ***C*** and ***G*** show immunolabeling for BrdU in the newborn cortex of wild-type and FKRP^{KD} mice following the intraperitoneal injection of BrdU into pregnant females at E15.5. Nuclei were counterstained with Hoechst 33342 (blue) and the merged images are shown in ***B*** and ***F***, and ***D*** and ***H***. Images were captured at 10× magnification. Scale bars, 200 μm.

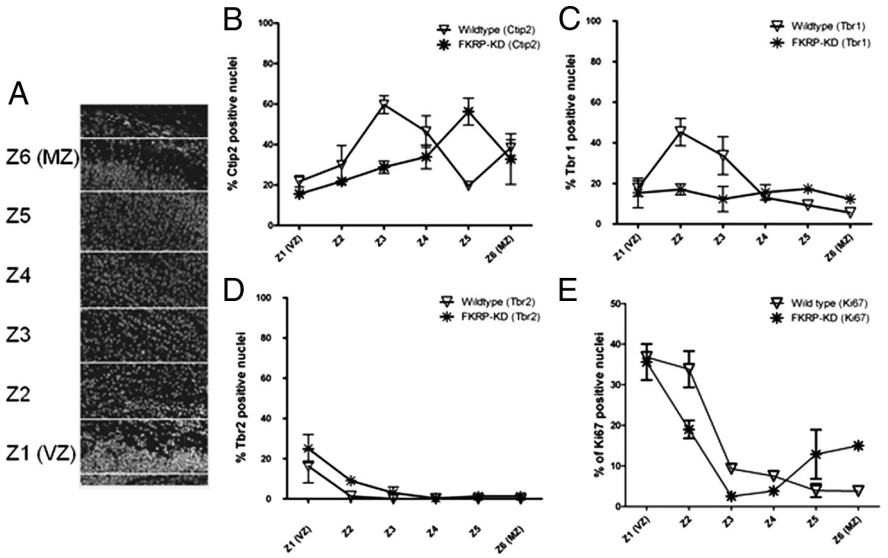

Figure 4. Distribution of cortical markers and proliferating cells across the cortical plate of FKRP^{KD} and wild-type brains. To quantify the distribution of specific population of neurons across the cortical plate of the FKRP^{KD} mice the cortical plate was arbitrarily divided into 6 equal divisions (***A***). The distributions of nuclei that were positive for staining with Ctip2 (***B***), Tbr-1 (***C***), Tbr-2 (***D***) and Ki67 (***E***) are plotted as a percentage of total nuclei.

Fkrp transcript levels are higher in the newborn mouse brain compared with skeletal muscle

Newborn FKRP^{KD} mice display a relatively mild muscle phenotype characterized by mild myopathic changes whereas the phenotype in the brain is associated with severe structural defects. We therefore sought to determine whether there was any evidence for a diverse requirement for FKRP during CNS development by assessing transcript levels in the newborn brain and muscle. The FKRP^{KD} ($n = 4$) mice showed an 80% reduction in *Fkrp* transcript levels in both tissues relative to wild type ($n = 3$) (Fig. 7*A*). *Fkrp* levels were found to be approximately fivefold higher in newborn brain relative to muscle following normalization to GAPDH ($n = 9$) (Fig. 7*A*). In contrast we observed no differences with respect to dystroglycan transcripts between brain and muscle (Fig. 7*B*).

Expression of laminin α1 and γ1 is increased in the brain but not in muscle of FKRP^{KD} mice

We previously reported a marked reduction in laminin α2 immunolabeling in both the brain and muscle of newborn FKRP^{KD} mice and have now demonstrated an ectopic distribution of laminin α1 in the brain of the FKRP-deficient animals. Since α-dystroglycan is known to have the capacity to bind to a number of laminin α-chains we sought to determine the levels of expression of laminin α1, α2, α3 α4, α5, and γ1. Quantification for each of these chains relative to endogenous GAPDH showed that while there was a trend for all the laminin α-chain mRNA expression to be increased in FKRP^{KD} brains when compared with wild type, only the data for laminin α1 and γ1 achieved statistical significance (Fig. 7*C*). By contrast in muscle where there is a milder phenotype at birth, no alteration in laminin α-chain (α2, α3 α4, α5, γ1) expression was observed between FKRP^{KD} and wild-type controls (data not shown).

Discussion

FKRP-null embryos die before reaching E12.5 (Chan et al., 2010). In our FKRP^{KD} mouse which displays an approximate 80% reduction in FKRP transcript levels, the muscle phenotype is relatively mild at birth, whereas that of the brain is characterized by a severe disruption in neuronal migration (Ackroyd et al., 2009). As antibodies to native FKRP are not available, we used RT-PCR to assess the relative levels of *Fkrp* gene expression. In newborn wild-type mice, brain *Fkrp* expression was approximately five times that in muscle, while analyses of dystroglycan expression showed no difference between the two tissues. On the basis of these data and the assumption that transcript expression reflects a difference in protein level these observations may be indicative of other protein targets in the brain or that dystroglycan processing in the brain is such that it requires different levels of *Fkrp* expression.

The ILM and pial basement membranes play crucial roles during eye and brain development, serving as attachment sites for the endfeet of the Müller glia and radial glia cells respectively (Halfter et al., 2005). Testament to this role is the abundance of cortical and retinal dysplasias in mice with defects in basement membrane components or receptors (Georges-Labouesse et al., 1998; Costell et al., 1999; De Arcangelis et al., 1999; Graus-Porta et al., 2001; Halfter et al., 2002; Beggs et al., 2003; Niewmierzycka et al., 2005; Haubst et al., 2006). The only laminin α-chain that was detectable at the ILM in the wild-type mice was α1. We previously demonstrated that IIH6 was not present at the newborn mouse ILM (Ackroyd et al., 2009); however, the glycosylated α-dystroglycan appears to be required earlier in development as the IIH6 epitope was detected at the ILM in the E12.5 wild-type eye. Since core α-dystroglycan is present at the ILM of newborn wild-type controls but is reduced or absent in FKRP^{KD} retina, our observations of a disturbance in this basement membrane suggests a defect in the dystroglycan:laminin α1 axis. Indeed a disruption of the dystroglycan:laminin α1 axis most likely causes a defect in Reichert's membrane and the embryonic lethality of FKRP (Chan et al., 2010), dystroglycan (Williamson et al., 1997) and fukutin-null mice (Kurahashi et al., 2005) support this hypothesis. We have not noted embryonic mortality in the FKRP^{KD} mice and assume that, as must be the case with POMGnT1-null and Large^{myd} mice, α-dystroglycan retains sufficient residual binding to laminin α1 to allow early basement membrane formation.

Cobblestone lissencephaly is characteristic of dystroglycanopathy patients at the severe end of the clinical spectrum and is caused by breaches in the pial basement leading to the formation of neuronal ectopias on the surface of the brain (Olson and Walsh, 2002). This is also seen in several dystroglycanopathy mouse models (Grewal and Hewitt, 2002; Hu et al., 2007). Evidence from other mouse models with defects in either laminin (Halfter et al., 2002) or integrin β1 (Radakovits et al., 2009) indicate that alterations in the formation of the pial basement membrane causes the radial glial cells to retract. At birth laminin α1, α2, and α5 are all present at the pial basement membrane of wild-type mice; however, in the FKRP^{KD} mouse laminin α2 and α5 were reduced at the pial surface while laminin α1, although not reduced, was "ectopically" located throughout the cortical plate. Whereas in other animal models for the dystroglycanopathies where breaches in the pial basement membrane are thought

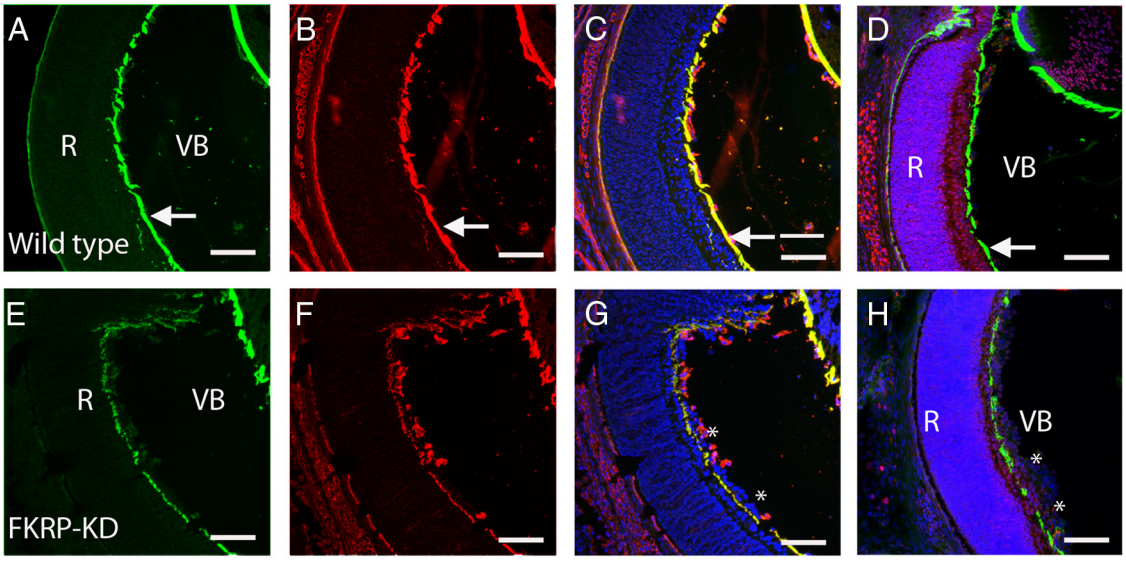

Figure 5. Irregular deposition of laminin α1 at the inner limiting membrane. ***A–H***, Coimmunostaining of wild-type (***A–D***) and FKRP^{KD} (***E–H***) for laminin α1 (green; ***A***, ***E***) and laminin 111/211 (red; ***B***, ***F***). The ILM (arrows) is juxtaposed between the retina and vitreous body in the wild-type controls. In the FKRP^{KD} retina this basement membrane is incomplete and ectopic nuclei from the ganglion cell layer (asterisk) of the retina are present in the vitreous body. Images ***C*** and ***G*** are merged images of ***A*** and ***B***, and ***E*** and ***F***, respectively. Costaining with RC2 to depict the Müller glia (red) and laminin α1 (green) demonstrate that in the retina of wild-type eye the Müller glia cell endfeet are anchored in the ganglion cell layer, juxtaposed with the ILM (***D***). In the FKRP^{KD} retina (***H***) the Müller glia endfeet penetrate through the incomplete basement membrane and are ectopically located in the vitreous body along with ectopically located ganglion cell nuclei. Nuclei are counterstained with Hoechst 33342 (blue). Scale bars, 50 μm.

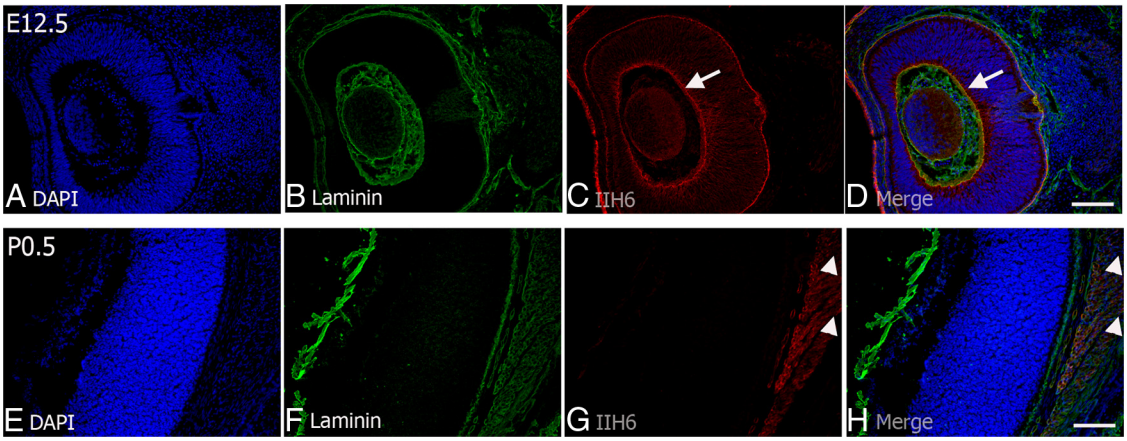

Figure 6. Glycosylated epitopes of α-dystroglycan are expressed at the ILM in a developmental regulated manner. Transverse sections (10 μm) of wild-type mouse eyes at ages E12.5 (***A–D***) and P0 (***E–H***) were immunolabeled with a polyclonal pan-laminin antibody (***B***, ***F***) or the IIH6 antibody (glycosylated α-dystroglycan; ***C***, ***G***). IIH6 staining is clearly present at the ILM of the E12.5 wild-type eye (arrows; ***C***, ***D***) but is not detected in the retina of newborn wild-type mice despite IIH6 immunoreactivity in the sarcolemma of the newborn eye (arrowheads; ***G***, ***H***). Nuclei were visualized with Hoechst 33342 (***A***, ***E***). Merged images are shown (***D***, ***H***). Scale bars, 50 μm.

to be caused by an overmigration of ectopic neurons (Hu et al., 2007) examination of the pial surface of the FKRP^{KD} mice indicates that the entire basement membrane had failed to form correctly. Indeed the radial glia in the FKRP^{KD} cortex often terminated at the sites of ectopic laminin α1 deposition. This ectopic deposition of laminin might be expected to disrupt both tangential and radial migration pathways, both of which are altered in patients and dystroglycanopathy mouse models (Holzfeind et al., 2002; Mercuri et al., 2006) and suggests an additional mechanism of disease with respect to the neuronal migration defect observed in patients at the severe end of the clinical spectrum. These observations are further supported by our analyses of BrdU incorporation in the FKRP^{KD} mice which show an accumulation of labeled cells within those areas broadly marked by the ectopic deposition of laminin rather than the marginal zone.

Since one consequence of a loss of adhesion to the basement membrane is the onset of apoptosis we investigated cell death in our FKRP^{KD} mice. However, no evidence was found of an increase in apoptosis in the FKRP^{KD} cortex relative to controls; we suggest that this could in part be due to the attachment of radial glial endfeet to the ectopic laminin deposits observed in the FKRP^{KD} cortex.

There was no evidence that proliferation (BrdU and Ki67 labeling) was altered in the cortex of the FKRP^{KD} relative to controls despite widespread disruption to the cortical lamination. Although the populations of Tbr2- and Ctip2-labeled neurons were unaffected the population of Tbr1-labeled neurons was significantly reduced in the FKRP^{KD} cortex. Tbr1 has recently been reported to impact on the cortical lamination as well as the development of the corticospinal tract (Han et al., 2011). Interestingly, abnormalities in the corticospinal tracts have previously

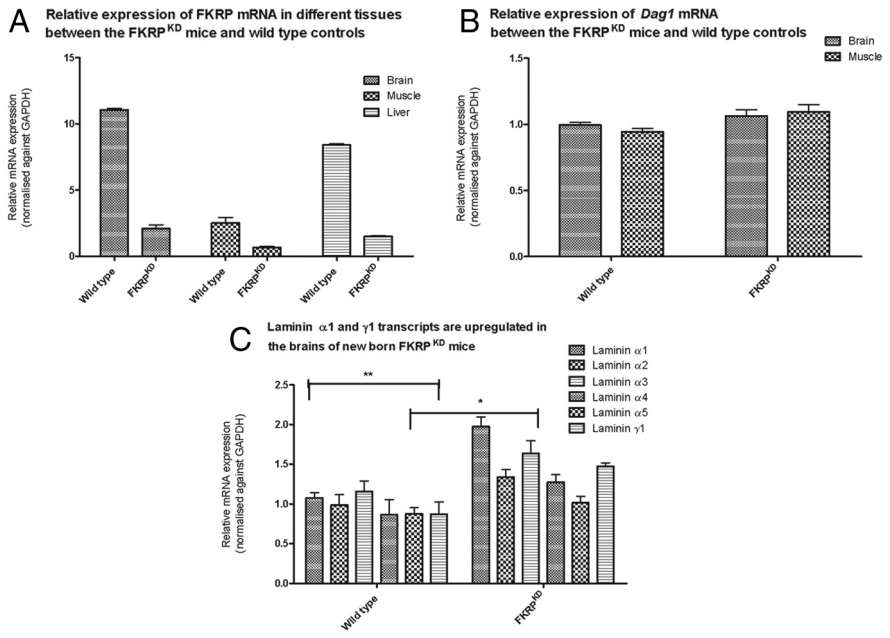

Figure 7. Real-time gene expression analysis of *Fkrp*, *Dag1*, and laminin in brain and muscle of newborn wild-type and FKRP ^{KD} mice. ***A***, Relative expression of FKRP. TaqMan (Applied Biosystems) RT-PCR probes were used to measure relative FKRP mRNA expression in brain, skeletal muscle and liver in the FKRP ^{KD} mice compared with age-matched wild-type controls. Expression levels were normalized against endogenous GAPDH mRNA expression. Error bars represent SEM ($n = 4$). All samples were analyzed as triplicate datasets. ***B***, Relative expression of dystroglycan. TaqMan (Applied Biosystems) RT-PCR probes were used to measure relative *Dag1* mRNA expression in brain and skeletal muscle in the FKRP ^{KD} mice compared with age-matched wild-type controls. Expression levels were normalized against endogenous GAPDH mRNA expression. Error bars represent SEM ($n = 3/4$). All samples were analyzed as triplicate datasets. ***C***, Laminin $\alpha1$ and $\gamma1$ mRNA is upregulated in the brain of the FKRP ^{KD} mice. TaqMan (Applied Biosystems) RT-PCR probes were used to measure relative laminin $\alpha1$, $\alpha2$, $\alpha3$, $\alpha4$, $\alpha5$, and $\gamma1$ mRNA expression in the brain of FKRP ^{KD} mice compared with age-matched wild-type controls. Expression levels were normalized against endogenous GAPDH mRNA expression. $^*p < 0.05$ (two-tailed *t* test); $^{**}p < 0.005$. Error bars represent $\pm$ SEM ($n = 3$). All samples were analyzed as triplicate datasets.

been indentified in MRI scans from human patients with a muscle-eye-brain-like phenotype (Clement et al., 2008b).

There were clear differences between the ILM and pial basement membrane of the FKRP ^{KD} mice; these related to the invasion of Müller glial processes through the ILM into the vitreous body and the absence of any obvious retraction of the Müller glia or ectopic laminin deposits. These differences may in part reflect the way each basement membrane forms, for example, the radial glial endfeet and the meningeal fibroblasts are thought to deposit the pial basement membrane on the surface of the brain, whereas the ILM forms by the precipitation of matrix proteins from the vitreous; a process thought to allow for the rapid assembly of the ILM during embryonic eye development (Halfter et al., 2008).

There is substantial evidence to show that retinal histogenesis is dependent on an intact ILM (Pinzón-Duarte et al., 2010). Mice lacking the nidogen binding site of the laminin $\gamma1$-chain and those deficient in laminin $\beta2/\gamma3$ have a structurally weakened ILM (Willem et al., 2002; Pinzón-Duarte et al., 2010). Tissue-specific patterns of glycosylation are thought to modify the laminin binding specificity of α-dystroglycan (McDearmon et al., 2006) and may effectively "customize" basement membranes in different locations. In agreement with this, brain and muscle α-dystroglycan have different molecular weights (120 and 156 kDa, respectively) and display different affinities for individual laminin α-chains, for example brain dystroglycan preferentially binds to laminin-511 and laminin-521 (McDearmon et al., 2006). Laminin $\alpha1$, $\alpha2$, and $\alpha5$ are present at the pial basement membrane, the presence of only laminin $\alpha1$ at the ILM demonstrates for the first time that a disturbance in the α-dystroglycan:laminin $\alpha1$ interaction contributes to the phenotype of the dystroglycanopathies.

Basement membranes typically self-assemble on cell surfaces; laminin binding to specific cell receptors which include α-dystroglycan and integrin $\beta1$ is fundamental to this process (Yurchenco and Patton, 2009). It has previously been shown that an absence of integrin $\beta1$ leads to a cessation of laminin $\alpha1$-chain synthesis (Aumailley et al., 2000). Moreover, it has been shown that neither integrin nor dystroglycan are uniquely required for basement membrane assembly; rather each is able to regulate their own expression and that of other basement membrane proteins (Li et al., 2002). This highlights an important feedback mechanism between the cell receptor and laminin gene expression which is supported by the upregulation that we observed in laminin $\alpha1$ mRNA. Expression of laminin $\alpha2$, $\alpha3$, $\alpha4$, and $\alpha5$ transcripts were also increased in the FKRP ^{KD} mice relative to wild type although this was not statistically significant. This may in part be due to the hypomorphic nature of our model.

In summary, we show that in the brain a reduction in *Fkrp* expression is associated with a marked disturbance in the deposition of several laminin α-chains and that an irregular deposition of laminin correlates with an inability of many of the radial glial to extend to the pial basement membrane. This disrupts both early and late-born neuronal migration and identifies a previously unrecognized mechanism of disease during brain development in the dystroglycanopathies. The observed defects in the ILM of the eye highlight the role of the dystroglycan: laminin $\alpha1$ axis in some of the eye defects seen at the severe end of the dystroglycanopathy spectrum. Since laminin $\alpha1$ and $\alpha2$ are the major isoforms in adult mouse tissues (Sasaki et al., 2002) these findings imply a functional redundancy in tissues not affected by the disease process. Overall our observations highlight aspects of the disease process which may impact upon the design of future therapeutic strategies.

References

Ackroyd MR, Skordis L, Kaluarachchi M, Godwin J, Prior S, Fidanboylu M, Piercy RJ, Muntoni F, Brown SC (2009) Reduced expression of fukutin related protein in mice results in a model for fukutin related protein associated muscular dystrophies. Brain 132:439–451.

Aumailley M, Pesch M, Tunggal L, Gaill F, Fässler R (2000) Altered synthesis of laminin 1 and absence of basement membrane component deposition in (beta)1 integrin-deficient embryoid bodies. J Cell Sci 113:259–268.

Barresi R, Campbell KP (2006) Dystroglycan: from biosynthesis to pathogenesis of human disease. J Cell Sci 119:199–207.

Beggs HE, Schahin-Reed D, Zang K, Goebbels S, Nave KA, Gorski J, Jones KR, Sretavan D, Reichardt LF (2003) FAK deficiency in cells contributing to the basal lamina results in cortical abnormalities resembling congenital muscular dystrophies. Neuron 40:501–514.

Beltrán-Valero de Bernabé D, Currier S, Steinbrecher A, Celli J, van Beusekom E, van der Zwaag B, Kayserili H, Merlini L, Chitayat D, Dobyns WB, Cormand B, Lehesjoki AE, Cruces J, Voit T, Walsh CA, van Bok-

hoven H, Brunner HG (2002) Mutations in the *O*-mannosyltransferase gene POMT1 give rise to the severe neuronal migration disorder Walker-Warburg syndrome. Am J Hum Genet 71:1033–1043.

Beltran-Valero de Bernabé B, Voit T, Longman C, Steinbrecher A, Straub V, Yuva Y, Herrmann R, Sperner J, Korenke C, Diesen C, Dobyns WB, Brunner HG, van Bokhoven H, Brockington M, Muntoni F (2004) Mutations in the FKRP gene can cause muscle-eye-brain disease and Walker-Warburg syndrome. J Med Genet 41:e61.

Bowe MA, Deyst KA, Leszyk JD, Fallon JR (1994) Identification and purification of an agrin receptor from Torpedo postsynaptic membranes: a heteromeric complex related to the dystroglycans. Neuron 12:1173–1180.

Brockington M, Blake DJ, Prandini P, Brown SC, Torelli S, Benson MA, Ponting CP, Estournet B, Romero NB, Mercuri E, Voit T, Sewry CA, Guicheney P, Muntoni F (2001a) Mutations in the fukutin-related protein gene (FKRP) cause a form of congenital muscular dystrophy with secondary laminin alpha2 deficiency and abnormal glycosylation of alpha-dystroglycan. Am J Hum Genet 69:1198–1209.

Brockington M, Yuva Y, Prandini P, Brown SC, Torelli S, Benson MA, Herrmann R, Anderson LV, Bashir R, Burgunder JM, Fallet S, Romero N, Fardeau M, Straub V, Storey G, Pollitt C, Richard I, Sewry CA, Bushby K, Voit T, et al. (2001b) Mutations in the fukutin-related protein gene (FKRP) identify limb girdle muscular dystrophy 2I as a milder allelic variant of congenital muscular dystrophy MDC1C. Hum Mol Genet 10:2851–2859.

Campanelli JT, Roberds SL, Campbell KP, Scheller RH (1994) A role for dystrophin-associated glycoproteins and utrophin in agrin-induced AChR clustering. Cell 77:663–674.

Chan YM, Keramaris-Vrantsis E, Lidov HG, Norton JH, Zinchenko N, Gruber HE, Thresher R, Blake DJ, Ashar J, Rosenfeld J, Lu QL (2010) Fukutin-related protein is essential for mouse muscle, brain and eye development and mutation recapitulates the wide clinical spectrums of dystroglycanopathies. Hum Mol Genet 19:3995–4006.

Clement EM, Godfrey C, Tan J, Brockington M, Torelli S, Feng L, Brown SC, Jimenez-Mallebrera C, Sewry CA, Longman C, Mein R, Abbs S, Vajsar J, Schachter H, Muntoni F (2008a) Mild POMGnT1 mutations underlie a novel limb-girdle muscular dystrophy variant. Arch Neurol 65:137–141.

Clement E, Mercuri E, Godfrey C, Smith J, Robb S, Kinali M, Straub V, Bushby K, Manzur A, Talim B, Cowan F, Quinlivan R, Klein A, Longman C, McWilliam R, Topaloglu H, Mein R, Abbs S, North K, Barkovich AJ, et al. (2008b) Brain involvement in muscular dystrophies with defective dystroglycan glycosylation. Ann Neurol 64:573–582.

Costell M, Gustafsson E, Aszódi A, Mörgelin M, Bloch W, Hunziker E, Addicks K, Timpl R, Fässler R (1999) Perlecan maintains the integrity of cartilage and some basement membranes. J Cell Biol 147:1109–1122.

De Arcangelis A, Mark M, Kreidberg J, Sorokin L, Georges-Labouesse E (1999) Synergistic activities of alpha3 and alpha6 integrins are required during apical ectodermal ridge formation and organogenesis in the mouse. Development 126:3957–3968.

Durbeej M, Larsson E, Ibraghimov-Beskrovnaya O, Roberds SL, Campbell KP, Ekblom P (1995) Non-muscle alpha-dystroglycan is involved in epithelial development. J Cell Biol 130:79–91.

Englund C, Fink A, Lau C, Pham D, Daza RA, Bulfone A, Kowalczyk T, Hevner RF (2005) Pax6, Tbr2, and Tbr1 are expressed sequentially by radial glia, intermediate progenitor cells, and postmitotic neurons in developing neocortex. J Neurosci 25:247–251.

Ervasti JM, Campbell KP (1993) A role for the dystrophin-glycoprotein complex as a transmembrane linker between laminin and actin. J Cell Biol 122:809–823.

Gee SH, Montanaro F, Lindenbaum MH, Carbonetto S (1994) Dystroglycan-alpha, a dystrophin-associated glycoprotein, is a functional agrin receptor. Cell 77:675–686.

Georges-Labouesse E, Mark M, Messaddeq N, Gansmüller A (1998) Essential role of alpha 6 integrins in cortical and retinal lamination. Curr Biol 8:983–986.

Godfrey C, Clement E, Mein R, Brockington M, Smith J, Talim B, Straub V, Robb S, Quinlivan R, Feng L, Jimenez-Mallebrera C, Mercuri E, Manzur AY, Kinali M, Torelli S, Brown SC, Sewry CA, Bushby K, Topaloglu H, North K, et al. (2007) Refining genotype phenotype correlations in muscular dystrophies with defective glycosylation of dystroglycan. Brain 130:2725–2735.

Graus-Porta D, Blaess S, Senften M, Littlewood-Evans A, Damsky C, Huang Z, Orban P, Klein R, Schittny JC, Müller U (2001) Beta1-class integrins regulate the development of laminae and folia in the cerebral and cerebellar cortex. Neuron 31:367–379.

Grewal PK, Hewitt JE (2002) Mutation of Large, which encodes a putative glycosyltransferase, in an animal model of muscular dystrophy. Biochim Biophys Acta 1573:216–224.

Halfter W, Dong S, Yip YP, Willem M, Mayer U (2002) A critical function of the pial basement membrane in cortical histogenesis. J Neurosci 22:6029–6040.

Halfter W, Willem M, Mayer U (2005) Basement membrane-dependent survival of retinal ganglion cells. Invest Ophthalmol Vis Sci 46:1000–1009.

Halfter W, Dong S, Dong A, Eller AW, Nischt R (2008) Origin and turnover of ECM proteins from the inner limiting membrane and vitreous body. Eye (Lond) 22:1207–1213.

Han W, Kwan KY, Shim S, Lam MM, Shin Y, Xu X, Zhu Y, Li M, Sestan N (2011) TBR1 directly represses Fezf2 to control the laminar origin and development of the corticospinal tract. Proc Natl Acad Sci U S A 108:3041–3046.

Haubst N, Georges-Labouesse E, De Arcangelis A, Mayer U, Götz M (2006) Basement membrane attachment is dispensable for radial glial cell fate and for proliferation, but affects positioning of neuronal subtypes. Development 133:3245–3254.

Henry MD, Campbell KP (1998) A role for dystroglycan in basement membrane assembly. Cell 95:859–870.

Henry MD, Williamson RA, Campbell KP (1998) Analysis of the role of dystroglycan in early postimplantation mouse development. Ann N Y Acad Sci 857:256–259.

Hevner RF, Shi L, Justice N, Hsueh Y, Sheng M, Smiga S, Bulfone A, Goffinet AM, Campagnoni AT, Rubenstein JL (2001) Tbr1 regulates differentiation of the preplate and layer 6. Neuron 29:353–366.

Hewitt JE (2009) Abnormal glycosylation of dystroglycan in human genetic disease. Biochim Biophys Acta 1792:853–861.

Holzfeind PJ, Grewal PK, Reitsamer HA, Kechvar J, Lassmann H, Hoeger H, Hewitt JE, Bittner RE (2002) Skeletal, cardiac and tongue muscle pathology, defective retinal transmission, and neuronal migration defects in the Large(myd) mouse defines a natural model for glycosylation-deficient muscle-eye-brain disorders. Hum Mol Genet 11:2673–2687.

Hu H, Yang Y, Eade A, Xiong Y, Qi Y (2007) Breaches of the pial basement membrane and disappearance of the glia limitans during development underlie the cortical lamination defect in the mouse model of muscle-eye-brain disease. J Comp Neurol 502:168–183.

Kurahashi H, Taniguchi M, Meno C, Taniguchi Y, Takeda S, Horie M, Otani H, Toda T (2005) Basement membrane fragility underlies embryonic lethality in fukutin-null mice. Neurobiol Dis 19:208–217.

Leid M, Ishmael JE, Avram D, Shepherd D, Fraulob V, Dollé P (2004) CTIP1 and CTIP2 are differentially expressed during mouse embryogenesis. Gene Expr Patterns 4:733–739.

Li S, Harrison D, Carbonetto S, Fassler R, Smyth N, Edgar D, Yurchenco PD (2002) Matrix assembly, regulation, and survival functions of laminin and its receptors in embryonic stem cell differentiation. J Cell Biol 157:1279–1290.

Liesi P (1990) Extracellular matrix and neuronal movement. Experientia 46:900–907.

Longman C, Brockington M, Torelli S, Jimenez-Mallebrera C, Kennedy C, Khalil N, Feng L, Saran RK, Voit T, Merlini L, Sewry CA, Brown SC, Muntoni F (2003) Mutations in the human LARGE gene cause MDC1D, a novel form of congenital muscular dystrophy with severe mental retardation and abnormal glycosylation of alpha-dystroglycan. Hum Mol Genet 12:2853–2861.

McDearmon EL, Combs AC, Sekiguchi K, Fujiwara H, Ervasti JM (2006) Brain alpha-dystroglycan displays unique glycoepitopes and preferential binding to laminin-10/11. FEBS Lett 580:3381–3385.

Mercuri E, Topaloglu H, Brockington M, Berardinelli A, Pichiecchio A, Santorelli F, Rutherford M, Talim B, Ricci E, Voit T, Muntoni F (2006) Spectrum of brain changes in patients with congenital muscular dystrophy and FKRP gene mutations. Arch Neurol 63:251–257.

Michele DE, Campbell KP (2003) Dystrophin-glycoprotein complex: post-translational processing and dystroglycan function. J Biol Chem 278:15457–15460.

Michele DE, Barresi R, Kanagawa M, Saito F, Cohn RD, Satz JS, Dollar J, Nishino I, Kelley RI, Somer H, Straub V, Mathews KD, Moore SA, Camp-

bell KP (2002) Post-translational disruption of dystroglycan-ligand interactions in congenital muscular dystrophies. Nature 418:417–422.
Muntoni F, Brockington M, Torelli S, Brown SC (2004) Defective glycosylation in congenital muscular dystrophies. Curr Opin Neurol 17:205–209.
Muntoni F, Brockington M, Godfrey C, Ackroyd M, Robb S, Manzur A, Kinali M, Mercuri E, Kaluarachchi M, Feng L, Jimenez-Mallebrera C, Clement E, Torelli S, Sewry CA, Brown SC (2007) Muscular dystrophies due to defective glycosylation of dystroglycan. Acta Myol 26:129–135.
Muntoni F, Torelli S, Brockington M (2008) Muscular dystrophies due to glycosylation defects. Neurotherapeutics 5:627–632.
Niewmierzycka A, Mills J, St-Arnaud R, Dedhar S, Reichardt LF (2005) Integrin-linked kinase deletion from mouse cortex results in cortical lamination defects resembling cobblestone lissencephaly. J Neurosci 25:7022–7031.
Olson EC, Walsh CA (2002) Smooth, rough and upside-down neocortical development. Curr Opin Genet Dev 12:320–327.
Peng HB, Ali AA, Daggett DF, Rauvala H, Hassell JR, Smalheiser NR (1998) The relationship between perlecan and dystroglycan and its implication in the formation of the neuromuscular junction. Cell Adhes Commun 5:475–489.
Pinzón-Duarte G, Daly G, Li YN, Koch M, Brunken WJ (2010) Defective formation of the inner limiting membrane in laminin beta2- and gamma3-null mice produces retinal dysplasia. Invest Ophthalmol Vis Sci 51:1773–1782.
Radakovits R, Barros CS, Belvindrah R, Patton B, Müller U (2009) Regulation of radial glial survival by signals from the meninges. J Neurosci 29:7694–7705.
Sasaki T, Giltay R, Talts U, Timpl R, Talts JF (2002) Expression and distribution of laminin alpha1 and alpha2 chains in embryonic and adult mouse tissues: an immunochemical approach. Exp Cell Res 275:185–199.
Sato S, Omori Y, Katoh K, Kondo M, Kanagawa M, Miyata K, Funabiki K, Koyasu T, Kajimura N, Miyoshi T, Sawai H, Kobayashi K, Tani A, Toda T, Usukura J, Tano Y, Fujikado T, Furukawa T (2008) Pikachurin, a dystroglycan ligand, is essential for photoreceptor ribbon synapse formation. Nat Neurosci 11:923–931.
Sorokin LM, Conzelmann S, Ekblom P, Battaglia C, Aumailley M, Timpl R (1992) Monoclonal antibodies against laminin A chain fragment E3 and their effects on binding to cells and proteoglycan and on kidney development. Exp Cell Res 201:137–144.
Sugita S, Saito F, Tang J, Satz J, Campbell K, Südhof TC (2001) A stoichiometric complex of neurexins and dystroglycan in brain. J Cell Biol 154:435–445.
Toda T (1999) [Fukutin, a novel protein product responsible for Fukuyama-type congenital muscular dystrophy.] Seikagaku 71:55–61.
Toda T, Kobayashi K, Takeda S, Sasaki J, Kurahashi H, Kano H, Tachikawa M, Wang F, Nagai Y, Taniguchi K, Taniguchi M, Sunada Y, Terashima T, Endo T, Matsumura K (2003) Fukuyama-type congenital muscular dystrophy (FCMD) and alpha-dystroglycanopathy. Congenit Anom (Kyoto) 43:97–104.
van Reeuwijk J, Janssen M, van den Elzen C, Beltran-Valero de Bernabé D, Sabatelli P, Merlini L, Boon M, Scheffer H, Brockington M, Muntoni F, Huynen MA, Verrips A, Walsh CA, Barth PG, Brunner HG, van Bokhoven H (2005) POMT2 mutations cause alpha-dystroglycan hypoglycosylation and Walker-Warburg syndrome. J Med Genet 42:907–912.
van Reeuwijk J, Grewal PK, Salih MA, Beltrán-Valero de Bernabé D, McLaughlan JM, Michielse CB, Herrmann R, Hewitt JE, Steinbrecher A, Seidahmed MZ, Shaheed MM, Abomelha A, Brunner HG, van Bokhoven H, Voit T (2007) Intragenic deletion in the LARGE gene causes Walker-Warburg syndrome. Hum Genet 121:685–690.
van Reeuwijk J, Olderode-Berends MJ, Van den Elzen C, Brouwer OF, Roscioli T, Van Pampus MG, Scheffer H, Brunner HG, Van Bokhoven H, Hol FA (2010) A homozygous FKRP start codon mutation is associated with Walker-Warburg syndrome, the severe end of the clinical spectrum. Clin Genet 78:275–281.
Whitmore C, Ackroyd M, Ashraf A, Brown SC (2011) Deposition of the inner limiting membrane of the eye of a mouse model for muscle-eye-brain disease. Neuromuscular Disord 21 [Suppl]:P17.
Willem M, Miosge N, Halfter W, Smyth N, Jannetti I, Burghart E, Timpl R, Mayer U (2002) Specific ablation of the nidogen-binding site in the laminin gamma1 chain interferes with kidney and lung development. Development 129:2711–2722.
Williamson RA, Henry MD, Daniels KJ, Hrstka RF, Lee JC, Sunada Y, Ibraghimov-Beskrovnaya O, Campbell KP (1997) Dystroglycan is essential for early embryonic development: disruption of Reichert's membrane in Dag1-null mice. Hum Mol Genet 6:831–841.
Yoshida A, Kobayashi K, Manya H, Taniguchi K, Kano H, Mizuno M, Inazu T, Mitsuhashi H, Takahashi S, Takeuchi M, Herrmann R, Straub V, Talim B, Voit T, Topaloglu H, Toda T, Endo T (2001) Muscular dystrophy and neuronal migration disorder caused by mutations in a glycosyltransferase, POMGnT1. Dev Cell 1:717–724.
Yoshida-Moriguchi T, Yu L, Stalnaker SH, Davis S, Kunz S, Madson M, Oldstone MB, Schachter H, Wells L, Campbell KP (2010) O-mannosyl phosphorylation of alpha-dystroglycan is required for laminin binding. Science 327:88–92.
Yurchenco PD, Patton BL (2009) Developmental and pathogenic mechanisms of basement membrane assembly. Curr Pharm Des 15:1277–1294.
Yurchenco PD, Amenta PS, Patton BL (2004a) Basement membrane assembly, stability and activities observed through a developmental lens. Matrix Biol 22:521–538.
Yurchenco PD, Cheng YS, Campbell K, Li S (2004b) Loss of basement membrane, receptor and cytoskeletal lattices in a laminin-deficient muscular dystrophy. J Cell Sci 117:735–742.